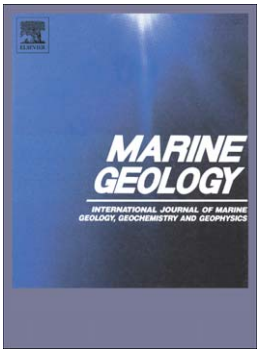

Composition and timing of carbonate vein precipitation within the igneous basement of the Early Cretaceous Shatsky Rise, NW Pacific

Sanzhong Li, Jörg Geldmacher, Folkmar Hauff, Dieter Garbe-Schönberg, Shan Yu, Shujuan Zhao, Svenja Rausch

PII: S0025-3227(14)00292-8
DOI: doi: 10.1016/j.margeo.2014.09.046
Reference: MARGO 5207

To appear in: *Marine Geology*

Received date: 23 August 2013
Revised date: 11 September 2014
Accepted date: 27 September 2014

Please cite this article as: Li, Sanzhong, Geldmacher, Jörg, Hauff, Folkmar, Garbe-Schönberg, Dieter, Yu, Shan, Zhao, Shujuan, Rausch, Svenja, Composition and timing of carbonate vein precipitation within the igneous basement of the Early Cretaceous Shatsky Rise, NW Pacific, *Marine Geology* (2014), doi: 10.1016/j.margeo.2014.09.046

Composition and timing of carbonate vein precipitation within the igneous basement of the Early Cretaceous Shatsky Rise, NW Pacific

Sanzhong Li[1,2], Jörg Geldmacher[3], Folkmar Hauff[3], Dieter Garbe-Schönberg[4], Shan Yu[1,2], Shujuan Zhao[1,2] , Svenja Rausch[5]

[1]College of Marine Geosciences, Ocean University of China, 266100 Qingdao, China

[2]Key Lab of Submarine Geosciences and Prospecting Technique, Ministry of Education, Qindao 266100, China

[3]GEOMAR Helmholtz Centre for Ocean Research Kiel, Wischhofstr. 1-3, D-24148 Kiel, Germany

[4]Institute of Geosciences, Christian-Albrechts University Kiel, Ludewig-Meyn Str. 10, D-24118 Kiel, Germany

[5]Geoscience Department, University of Bremen, Klagenfurter Str., 28359 Bremen Germany

Corresponding author: Jörg Geldmacher, GEOMAR Helmholtz Centre for Ocean Research Kiel, Wischhofstr. 1-3, D-24148 Kiel, Germany

Phone: +49 431 600-2260, jgeldmacher@geomar.de

Abstract

Numerous calcium carbonate veins were recovered from the igneous basement of the Early Cretaceous Shatsky Rise during Integrated Ocean Drilling Program (IODP) Expedition 324. The chemical (Sr/Ca, Mg/Ca) and isotopic ($^{87}Sr/^{86}Sr$, $^{143}Nd/^{144}Nd$, $\delta^{18}O$, $\delta^{13}C$) compositions of these veins were determined to constrain the timing of vein formation. A dominant control by seawater chemistry on calcite composition is evident for most vein samples with variable, contributions from the basaltic basement. Slightly elevated precipitation temperatures (as inferred from oxygen isotope ratios), indicative of hydrothermal vein formation, are only observed at Site U1350 in the central part of Shatsky Rise. The highest $^{87}Sr/^{86}Sr$ ratios (least basement influence) of vein samples at each drill site range from 0.70726 to 0.70755 and are believed to reflect the contemporaneous seawater composition during the time of calcite precipitation. In principle, age information can be deduced by correlating these ratios with the global seawater Sr isotope evolution. Since the Sr isotopic composition of seawater has fluctuated three times between the early and mid Cretaceous, no unambiguous precipitation ages can be constrained by this method and vein precipitation could have occurred at any time between ~80 and 140 Ma. However, based on combined chemical and isotopic data and correlations of vein composition with formation depth and inferred temperature, we argue for a rather early precipitation of the veins shortly after basement formation at each respective drill site.

Keywords: IODP, Expedition 324, JOIDES Resolution, Shatsky Rise, calcite vein, strontium isotope ratio, $\delta^{18}O$

1. Introduction

The circulation of seawater through igneous oceanic crust and both the dissolution of elements by, and precipitation from these fluids within the basement rocks, comprise major aspects of global element budgets including the long-term carbonate cycle (e.g. Brady and Gislason 1997; Alt and Teagle, 1999; Coggon et al., 2010). The isotopic and chemical signature of seawater, e.g. ratios of dissolved cations or Sr isotopic composition, varies over geological time and reflects global changes in the Earth environment. The systematic changes of $^{87}Sr/^{86}Sr$, as recorded in marine carbonates, have long been used for constraining the ages of marine limestones and fossil carbonate shells (e.g. Peterman et al., 1970, Burke et al., 1982). Carbonate minerals that were precipitated from fluids that circulate through cracks and cavities and form calcium carbonate veins in the igneous upper oceanic crust are seldom considered in this regard since they form in direct interaction with the basement rocks and can contain a significant lithospheric (often hydrothermal) contribution. Recently, however, it was shown that important seawater parameters (Sr isotopic composition, Mg/Ca, Sr/Ca ratios) are reliably recorded in calcium carbonate veins, if precipitated at near ambient seawater temperature (Coggon et al., 2004; Coggon et al., 2010, Rausch et al., 2013) or can be reconstructed if the precipitation temperature is known (Coggon and Teagle, 2011). In this paper we report Mg/Ca and

Sr/Ca ratios, trace element and isotopic compositions ($^{87}Sr/^{86}Sr$, $^{143}Nd/^{144}Nd$, $\delta^{18}O$, $\delta^{13}C$) of carbonate veins drilled at four sites of different age on Shatsky Rise, a large oceanic plateau formed in the early Cretaceous in the NW Pacific. The global seawater Sr-isotope stratigraphy will be used to discuss possible vein precipitation ages, which in turn can be compared with measured or assumed basement formation ages. In addition, the data provide insights into fluid circulation and alteration history of one of the oldest *in-situ* oceanic plateaus on Earth.

2. Regional geology and previous work

Shatsky Rise is a Large Igneous Province located in the NW Pacific ca. 1500 km east of Japan (Fig. 1) and is the third-largest oceanic plateau (after Ontong Java and Kerguelen) in the present oceans. Based on paleomagnetic reversals combined with bathymetric data, the plateau's three main volcanic edifices Tamu, Ori and Shirshov massifs are proposed to have successively formed by massive volcanism along a southwest-northeast moving, rapidly spreading triple junction (Nakanishi et al., 1999). The enormous size of the plateau (~4.8×10^5 km^2 comprising ~4.3×10^6 km^3 basalt, Sager et al., 1999) and the apparent decrease in effusive activity with time, however, would be also consistent with a formation by a (starting) mantle plume head (e.g. Sager, 2005). The proposed NW-directed age progression across Shatsky Rise is solely based on the interpretation of magnetic reversals since only a single radiometric age determination of basement rock from the southern flank of Tamu Massif was published so far (144.6±0.8 Ma, Mahoney et al., 2005). During IODP Expedition 324,

volcanic basement was cored near the Tamu summit (Site U1347, ~318 m penetration, thereof 160 m into igneous basement), Ori summit (U1349, ~250 m, thereof 165 m basement), Ori's lower flank (U1350, 316 m, thereof 143 m basement) and Shirshov summit (U1346, 192 m, thereof 140 m into basement). Recent and/or preliminary $^{40}Ar/^{39}Ar$ age determinations yield ages of 143.1 (±3.3) Ma and 144.4 (±1.0) Ma for the bulk of lavas drilled at Tamu Site U1347 (Geldmacher et al., in press) and an age of 134.1(±1.0) Ma for a lava recovered at U1350 from the upper flank of Ori (Heaton and Koppers, 2014). Ages inferred from the respective youngest magnetic seafloor anomalies imply similar or slightly older ages for these sites (M19=144 and M14=136 Ma, respectively, Nakanishi et al. 1999).

The drilled igneous units comprise pillow lavas (0.2-1.0 m diameter), pillow-like inflation units (0.8-2.0 m thick), small massive flow units (~2-4 m) and large massive flow units (~5-23 m) (Sager et al., 2010). All basement rocks have tholeiitic composition, similar to mid ocean ridge basalts (MORB) with plagioclase and clinopyroxene being the main crystal phases. The rocks have undergone varying degrees of fluid-rock alteration with predominant changes resulting from interaction of basalt with seawater-derived fluids under anoxic-suboxic conditions at low temperature and low water-rock ratios. Certain primary phases (olivine, glassy mesostasis) are commonly replaced by clay minerals i.e. smectite and sapponite (Sager et al., 2010). Generally, the lavas show more extensive alteration at volcano summit sites (U1346, U1349) compared to flank sites (U1347, U1350), indicating that

summit structures (and sustained heat at the volcano center) promoted fluid flow. Site U1346 lavas from Shirshov Massif are particular altered with most primary phases being replaced by secondary minerals. Regular veins (extensional fractures filled with secondary minerals) are common at all sites but particularly in lavas with fine-grained groundmass and low vesicularity. Most veins are 0.1 to 3 mm thick (maximum width can reach 10 mm) and are generally filled with calcite, although the fill can vary from oxyhydroxide/phyllosilicate material at the edges to calcite in the vein center (Sager et al., 2010). Calcite-rich veins commonly show polycrystalline fabrics and often syntaxial or cross-fiber texture. Veins filled with pyrite are also observed (particular at Site U1350) but pyrite-filled veins are generally much thinner (0.1-1mm). Vein density ranges from 3 veins/m downhole (U1346, U1347) to 6.1 and 6.6 veins/m (U1350 and U1349). Veins are particular abundant at the Ori Sites (U1349, U1350), possibly indicating that Ori Massif experienced stronger contractional stress than the two other massifs (Sager et al., 2010). These numbers are comparable to other oceanic crust segments of Jurassic age (e.g., 170 Ma MORB at Site 801 off the Mariana Trench= 6.1 veins/m, Rausch et al., in prep.) but less than the reported 18-30 veins/m for the Cretaceous Ontong Java Plateau (Banerjee and Honnorez, 2004).

3. Sampling, sample preparation and analytical methods

Representative veins from all Exp. 324 sites (that reached the volcanic basement) were selected based on visual core description and microscopic thin section observation. The selected veins cover a variety of depth intervals within the basement

(from 3.9 m below the top of the igneous basement down to 147 m within the lava pile). The filling material of calcium carbonate veins (calcite) was obtained by handpicking from crushed core material. Mechanical sample preparation was carried out at the Institute of Geology and Mineral Survey, Hebei Province, China.

Sr/Ca, Mg/Ca and trace element composition were measured at the Institute of Geosciences, University Kiel, Germany. Approximately 100 mg sample particles were digested in 5 ml hot (130°C) concentrated HNO_3. Other acids (e.g. HCL, HF) were not used to ensure that only carbonate phases (and no possible basaltic wall rock contaminants) contribute to the data. The solution was centrifuged, dried up and collected with 1 ml 8N HNO_3. An aliquot of this solution was 100-200fold diluted with 2% (v/v) subb. HNO_3, and spiked with 2.5 ppb Be, In, Re for internal standardization. Trace elements (Li, Sc ,Mn, Rb, Sr, Ba, Pr, Pb, U, Y and all REEs) were measured by inductively coupled plasma-mass spectrometry (ICP-MS) on an Agilent 7500cs instrument. Additionally, international carbonate standards JCP-1 and JLs were digested and Sr concentration was found within ±4% rel. of the preferred value. Replicate measurements show a precision of better than 1% RSD for most elements (including Sr) except Sc, Mn, Rb, Y, Ba, La, (1-6%) and Li (15% RSD). Measurements of duplicate digests differ by less then 5% for most elements except Li, Sc, Rb, Ba and Pb. Additionally, the element ratios Mg/Ca and Sr/Ca were measured in high-precision mode by inductively coupled plasma-optical emission spectroscopy (ICP-OES) on a SPECTRO Ciros^{CCD} SOP in the same laboratory combining

analytical procedures of Schrag *(*1999) and de Villiers et al. (2002). An in-house coral standard (*Mayotte 5a*, 8.9916 mmol/mol Sr/Ca) bracketing every batch of 6 samples was used for instrumental drift correction which was typically <2%rel. Average internal error of 5 replicate Sr/Ca determinations per sample is <0.08% RSD. External error of Sr/Ca ratios estimated from replicate measurements on the same day and on consecutive days is <0.09% RSD. Accuracy was monitored by analyzing the *Porites* coral standard JCp-1 as an unknown giving Sr/Ca 8.858 ± 0.011 mmol/mol (n=4), which compares to 8.838 ± 0.089 mmol/mol as average from an international inter-laboratory comparison (Hathorne et al., 2013).

Isotopic ratios were determined both at the Institute of Geology and Geophysics, China Academy of Sciences IGGCAS ($^{87}Sr/^{86}Sr$) and at GEOMAR Helmholtz Centre for Ocean Research Kiel, Germany ($^{87}Sr/^{86}Sr$ and $^{143}Nd/^{144}Nd$) by thermal ionisation mass spectrometry (TIMS). At GEOMAR, chemical separation procedures followed the method outlined in Hoernle and Tilton (1991) and Sr and Nd isotopic ratios were measured on a Finnigan MAT 262 (Sr) and TRITON TI (Nd). All analyzes were fractionation-corrected within-run to $^{86}Sr/^{88}Sr$ of 0.1194 and $^{146}Nd/^{144}Nd$ of 0.7219. Repeated measurements of Sr isotope standard NBS987 (n=11) yielded 0.710250±8 (2 sigma). The La Jolla Nd standard averaged 0.511850±6 (n=5). Results of replicate analyses are given in Table 1. The $^{86}Sr/^{88}Sr$ ratios of the carbonate standards JCp-1 and JLs-1 that were run with the samples, averaged at 0.709160 and 0.707813 respectively, in good agreement with literature data for JCP-1 (0.709150-0.709164,

Okai et al., 2002) and with slight deviation for JLs-1 (0.707850, Terashiwa et al., 1990). At IGGCAS, approximately 100 mg of carbonate material was dissolved on a hotplate at 80°C using 2.0 mL of 0.2 M HCl for 2 hours. After centrifugation, the supernatant was picked up and dried on a hotplate. The samples were re-dissolved with 1.0 mL of 2.5 M HCl. Then, the sample solution was loaded onto the pre-conditioned column with 2 mL of AG50W×12 (200-400 mesh) and Sr was separated from the sample matrix following the procedure outlined in Li et al. (2012) and Yang et al. (2010). The whole procedure blank was lower than 300 pg for Sr. The Sr isotopic measurements were performed on a Finnigan MAT262 TIMS at IGGCAS. A double Re filament configuration was used and Sr isotope data were acquired in the static collection mode. The mass fractionation of Sr was corrected using exponential law with $^{86}Sr/^{88}Sr=0.1194$. International standard sample NBS-987 was employed to evaluate instrument stability during the period of data collection. During the data collection period, the measured average value of the NBS987 was $^{87}Sr/^{86}Sr = 0.710234 \pm 0.000013$, in good agreement with the reported values (Li et al., 2012, Yang et al., 2010) and well within error of the NBS987 measurements at GEOMAR. As shown in Table 1 duplicate samples digested and measured at the Institute of Geology and Geophysics, China and at GEOMAR generally overlap within analytical error of each other.

Stable oxygen and carbon isotope ratios of calcites were measured on a Finnigan MAT 253 mass spectrometer system equipped with a Kiel IV Carbonate Preparation

Device at the GEOMAR Stable Isotope Lab. The carbonate was treated with orthophosphoric acid at ca 70°C. For each sample three to five measurements were carried out using about 5 individual calcite grains (150-250 μm) per measurement. Average isotope values of individual runs are given in Table 1. The analytical accuracy was <0.03‰ for $\delta^{13}C$ and <0.06‰ for $\delta^{18}O$. All measurements were calibrated to Pee Dee Belemnite standard using NBS 19.

4. Results

4.1 Elemental composition

All vein samples show relatively low Sr concentrations averaging 190 ppm (range 57-629 ppm, n=18) resulting in low Sr/Ca ratios (0.06 to 0.81 mmom/mol) being characteristic for calcite. In contrast, aragonite has high Sr (~4000 ppm) with considerably lower Mg concentration (Coggon et al. 2004). The Sr/Ca ratio of the vein calcite is positively correlated with Mg/Ca (Fig. 2) as observed in previous studies of relatively young (few million years) carbonate veins. This relationship has been explained by the enhanced incorporation of the slightly larger Sr^{2+} ion into the calcite crystal lattice (substituting for Ca) after incorporation of the slightly smaller Mg^{2+} ion has increased the available size of the neighboring sites (Mucci and Morse, 1983; Rausch et al., in prep.). On a Post-Archean Australian Shale (PAAS)-normalized plot of rare earth elements (REE) and Y, the samples show relatively similar-shaped patterns although concentrations of individual elements can vary by almost two magnitudes (Fig. 3). Light REE are relatively depleted compared

to the heavy REE which display less fractionated, almost horizontal patterns. Several samples show characteristic anomalies for the multivalent elements Ce and Eu, which can be segregated from other REE's by oxidation-reduction processes involving seawater (see below). The investigated calcite vein samples show variable Ce depletion (defined as Ce/Ce* =2xCe/(La+Pr)). Although only one sample from Ori summit (U1349A-11R-5) shows a strong Ce trough with $(Ce/Ce^*)_n$=0.22 (Fig. 3), most samples yield weak negative anomalies having $(Ce/Ce^*)_n$ <1 (Fig. 4c). Only one sample from Ori flank (U1350A-23R-3) shows a slight Y enrichment but has a less pronounced Ce depletion compared to the Ori summit sample U1349A-11R-5. In PAAS normalized diagrams, all of our calcite samples display a positive Eu anomaly (Eu*=Eu/√(Sm*Gd)) with only one exception. This is, however, a result of normalization to PAAS which itself has a negative Eu-anomaly when normalized to chondrite. Basalts from the Shatsky Rise usually do not have a Eu anomaly in chondrite-normalized patterns but, consequently, display a positive Eu anomaly when normalized to PAAS. This effect is mirrored by the calcites being precipitated from fluids that equilibrated during basalt-seawater interaction: almost all samples have a negative Eu anomaly after chondrite normalization (not shown). There is, however, one sample U1349A-7R-4 from Ori summit that has a positive Eu anomaly even in a chondrite-normalized plot suggesting some influence from ancient high-temperature hydrothermal activity at this site.

4.2 Isotopic composition

Measured $^{87}Sr/^{86}Sr$ and $^{143}Nd/^{144}Nd$ isotopic ratios of the calcite veins range from 0.706518 to 0.707550 and 0.513016 to 0.513290 respectively (Figs. 4a, d). Whereas the range of Nd isotopic ratios of the calcite veins partly overlaps with the range of lavas at Shatsky (0.512969 to 0.513237), their Sr isotope ratios are all considerably higher than those of the lavas (0.702650 to 0.703345, excluding strongly altered lavas, Heydolph at al., 2014). In fact, the Sr isotope ratios of most samples overlap or are very close to Early Cretaceous seawater composition (Fig. 4d). No clear correlations of calcite vein $^{87}Sr/^{86}Sr$ isotopic ratios with most geochemical parameters such as Ce/Ce*, Eu*, Mg/Ca e.g. are observed. Sr/Ca (Fig. 4b) and Mg/Ca and Y/Y* (=Y/√(Dy*Ho)), however, are weakly negative correlated with $^{87}Sr/^{86}Sr$, displaying concavely-shaped trends (not shown).

The $^{18}O/^{16}O$ and $^{13}C/^{12}C$ isotope data are reported relative to PDB by using the delta notation ($\delta^{18}O$, $\delta^{13}C$) and are presented in Table 1. The $\delta^{18}O$ values range from 1.44 (Tamu sample U1347A-27R-6) to -3.30 (Ori flank sample U1350A-22R-2). When considering the sites individually, veins from Tamu and Ori summit show a relative narrow range of $\delta^{18}O$ values (~1 ‰) whereas veins from the Shirshov and Ori flank sites show a wider spread (3-4‰). The $\delta^{18}O$ values are positively correlated with Mg/Ca and Sr/Ca as also seen in Fig. 2. No correlation with other trace element parameters is observed, pointing to a rather complex origin of the oxygen isotope record in the vein samples (see section 5.3). The $\delta^{13}C$ values from the individual drill sites show a narrow spread (except for U1350) averaging at 0.46 (U1346), -0.74

(U1347), and 0.91 (U1349). In contrast, $\delta^{13}C$ values from U1350 range from -0.78 to -5.8.

5. Discussion

5.1 Controls on vein composition

The REE and Y concentrations can be used to evaluate seawater involvement in carbonate vein formation. Seawater is typically depleted in Ce (negative anomaly relative to neighboring La_N and Pr_N), whereas Eu can get enriched in hydrothermal fluids showing a positive Eu anomaly (e.g. Nozaki, 2001). Yttrium, often included with the REEs because of its similar chemical behavior, is slightly enriched in seawater compared to Dy_N and Ho_N (Zhang and Nozaki, 1996). Calcites precipitating from fluids influenced by extensive seawater-basalt exchange are therefore often characterized by the absence of negative Ce and absence of positive Y anomalies (e.g., Rausch et al., submitted). In this regard, the investigated vein samples display indicators for both seawater derivation ($Ce/Ce^*<1$) and interaction with the basaltic host rock (relative Eu enrichment, chondritic Y/Ho), suggesting that the fluids from which the calcite was precipitated were formed by variable degrees of seawater-basalt interaction and with variable involvement of individual elements even in the same vein sample. Considering the radiogenic isotope systems Nd and Sr, a quantitative approach was applied: As shown by the simple, binary mixing model in Fig. 4d, the igneous basement contribution is ≤1% for the less influenced veins from Sites U1349 and U1346, and only slightly higher for most other investigated veins. Instead a

dominant control of seawater Sr (>98%) on the vein composition is indicated. Although a simple mixing model is not fully appropriate to describe the extent of exchange between differently fluid-mobile elements/isotopes, it does provide minimum estimates.

5.2 Timing of vein formation based on Sr isotope data

In principle, the Sr isotopic composition of seawater derived carbonate phases can be used to constrain their formation age (e.g. McArthur et al., 2001). Strontium is easily mobilized and leached from the basaltic basement but is also abundant in seawater (modern value: ~7.8 ppm but there is evidence that the seawater Sr content may have been ≥38 ppm in the Cretaceous, Coogan, 2009). Seawater Sr is readily incorporated into precipitating calcite (substituting for Ca) and since the $^{87}Sr/^{86}Sr$ isotopic composition of seawater has varied over geological time (e.g. Peterman et al., 1970; Hart and Staudigel, 1978; Veizer et al., 1999; McArthur et al., 2001), the Sr isotopic ratio of the veins can potentially determine the time of carbonate precipation. However, any contribution of Sr leached from the basaltic basement will lower the Sr isotopic composition of the vein calcite since oceanic basalts have a much less radiogenic $^{87}Sr/^{86}Sr$ ratio (Fig. 4d). As shown in Fig. 4a, calcite veins that precipitated deeper in the basement yield systematically lower $^{87}Sr/^{86}Sr$ ratios. If the veins precipitated long after the eruption within a cold basement, such correlation could reflect an increase of basaltic influence with increasing distance that the seawater had to travel through the basaltic matrix. Alternatively, if the veins were formed shortly

after lava emplacement from seawater-derived hydrothermal fluids interacting with the hot basalt in deeper levels of the lava pile, this correlation could reflect either increasing intensity of basalt-seawater interaction under increasing (magmatic) temperatures with depth and/or the diluting effect of seawater to hydrothermal fluids that migrate upwards in the basement pile and approach pristine seawater at the top of the basement. The only sample group that does not seem to follow this correlation are veins from Site U1350, located on the lower flank of the Ori edifice.

Additional complexity for constraining the formation age of the veins by correlating their Sr isotope ratios with the seawater evolution curve arises from the fact that the $^{87}Sr/^{86}Sr$ composition of seawater has fluctuated three times between the Early and Mid Cretaceous (Fig. 5). If the most radiogenic (highest) $^{87}Sr/^{86}Sr$ calcite ratios at each respective volcanic edifice (also equivalent to the shallowest veins measured from the top of the basement at each drill site - compare Fig. 4a) are considered to reflect the most pristine seawater signal, veins from the three edifices could have formed at different times between ~80 and 140 Ma respectively (intersection of stippled lines with the seawater Sr curve in Fig. 5). Interestingly, the respective highest Sr isotope ratios of the calcite veins at each edifice increase with the presumed decreasing age of the respective edifice. If samples are arranged according to preliminary age determinations and assumed ages of their host lavas (with a highest possible age of ~143 Ma for Tamu, and ~134 Ma for Ori (see chapter 2: Regional geology and previous work), the increase of the highest Sr isotope ratios at each

respective site seems to mimic the Sr isotopic increase of the respective contemporaneous seawater. No radiometric ages for lavas from Shirshov Site U1346 are available yet, but a minimum (youngest) age of ~128 Ma is inferred from calcereous nannofossil assamblages within the sediment pile immediately overlying the volcanic basement (Sager et al., 2010). The observed systematic increase of the highest calcite $^{87}Sr/^{86}Sr$ ratios at each edifice corresponding to a similar increase in $^{87}Sr/^{86}Sr$ seawater composition, could therefore reflect the assumed decreasing age of the three Shatsky edifices. This would point towards a rather early formation of the veins, contemporaneous to, or within a few million years after lava emplacement (see below). In contrast, if the veins would have formed much later (e.g. in the Mid- or Late Cretaceous) such a systematic correlation of $^{87}Sr/^{86}Sr$ with decreasing basement age would not be expected and difficult to explain.

In addition, if the vein network formed in an open system with fresh seawater percolating over an extended period of time, a typical seawater signature with pronounced negative Ce anomaly (Ce/Ce* <0.8) and positive Y and Gd anomalies would be expected in the vein's calcite composition. In contrast, the lack of these characteristic anomalies is expected for veins with low $^{87}Sr/^{86}Sr$ ratios indicative of increased interaction with basaltic basement under suboxic/anoxic conditions and limited exchange with seawater (Rausch et al. in prep.). As shown in Fig. 4c, the composition of most samples, showing no pronounced Ce anomalies (Ce/Ce* of our samples = >0.8 to 1), suggests more closed formation conditions with restricted fresh

supply of fully oxidized circulating seawater.

The highest $^{87}Sr/^{86}Sr$ ratio of all veins from Tamu massif is 0.707264±13 (U1347A-16R-5, 119-123 cm), a value that was reached for the first time by seawater at ~141.2 Ma, well within the analytical error of the radiometric age determination of the host lava (143.1±3.3) for this site. The highest $^{87}Sr/^{86}Sr$ ratio of all veins from Ori edifice is 0.707455±7 (U1349A- 7R-4, 7.2-16 cm), a value that was reached for the first time by seawater at 132.1 Ma, which is just about 2 million years younger than the only available preliminary age from Ori (from the flank of this seamount) of 134±1 Ma. This value was then exceeded by seawater during the first Cretaceous Sr isotope seawater fluctuation until ~125 Ma. Similarly high Sr isotope seawater values were not reached again before ~105 Ma (McArthur et al. 2001, Fig. 5). The highest $^{87}Sr/^{86}Sr$ ratio from a Shirshov vein is 0.707550 (U1346A-10R-2, 50-57 cm, average value of two measurements) plotting slightly above the statistically best-fit seawater Sr curve (at 95% confidence bound) at ~128 Ma. This high value was analytically re-confirmed by processing and measuring calcite fillings from this vein at both GEOMAR and OUC (see Table 1). Comparable high $^{87}Sr/^{86}Sr$ values are not reached again before ~78 Ma, at times when the basement at this drill site is already covered by >>60 meters of pelagic sediment (Sager et al., 2010) inhibiting seawater circulation. However, assigning this value to the peak of the first Cretaceous Sr seawater fluctuation at around 128 Ma, which corresponds well with the palaeontologically constrained minimum basement age of around 128 Ma (see above),

needs to be regarded with caution. Some influence of younger (<78 Ma) seawater cannot be ruled out for this sample.

Considering the veins with Sr isotope ratios lower then seawater value at 143, 134 and 128 Ma at the respective sites, indicating various contributions of unradiogenic Sr from the basaltic host rocks, a co-genic formation with the veins reflecting contemporaneous seawater Sr can only be assumed. This assumption is supported by the positive correlation of Sr isotopic ratio and formation depth within the basement (Fig. 4a) for veins from Sites U 1347 (Tamu) and U1349 (Ori summit). For Shirshov Site U1346, however, this relationship is less clear with two samples (U1346A-10R-2 and U1346A-16R-1) having elevated Sr isotope ratios in respect to their formation depth. Since sample U1346A-10R-2 yields the aforementioned Sr isotope ratio higher than seawater at any time before ~78 Ma, a younger compositional overprint for this vein is substantiated.

5.3 Further constraints on vein formation from oxygen isotope data

The oxygen isotopic composition, expressed in $\delta^{18}O$, of authigenic carbonate minerals depends on precipitation temperature (and the $\delta^{18}O$ of the oxygen source) and is an established proxy for seawater temperature (see Grossman, 2012 for overview). Based on recent (<4 Ma) carbonate veins at Juan de Fuca Ridge, Coggon et al. (2004) have shown that carbonates precipitating from hotter fluids with enhanced basaltic $^{87}Sr/^{86}Sr$ contribution have lower Sr/Ca and Mg/Ca concentrations. This proposed relationship

is generally confirmed by the Cretaceous Shatsky vein data (Fig. 2), having lower (warmer) $\delta^{18}O$ values with decreasing Sr/Ca and Mg/Ca ratios and vice versa. In addition, vein samples with the highest $^{87}Sr/^{86}Sr$ ratios at each respective site yield $\delta^{18}O$ values that overlap or are most similar to Early Cretaceous seawater oxygen isotopic composition (Grossmann, 2012) at the assumed ages of 143, 134 and 128 Ma for the respective edifices (Fig. 6a). The lesser the veins Sr isotopic composition deviates from the seawater curve, the more similar are their oxygen isotope ratios to contemporaneous seawater, which is believed to have $\delta^{18}O$ values around zero between 128 to 143 Ma (based on fossil belemnite data, see compilation in Grossman, 2012). Such values would correspond to precipitation (water) temperatures of about 10°C (assuming equilibrium precipitation) or 17 °C (non-equilibrium, equations of Kim and O'Neil, 1997) (see Fig. 6 caption for details). Both estimates are well reasonable considering that Shatsky Rise was formed at the equator (Tominaga et al., 2012) with the basement tops reaching up to intermediate or relative shallow (neritic) water depths (Sager et al., 2010).

Veins that possess higher $\delta^{18}O$ values than Early Cretaceous seawater (indicating that they were formed at 1° to 5° C lower temperatures) also show slightly lower $^{87}Sr/^{86}Sr$ ratios (two samples from U1347 and one sample from U1346 and U1349 respectively). There seems to be a relationship of higher $\delta^{18}O$ values (slightly colder) and lower $^{87}Sr/^{86}Sr$ ratios with increasing sample depth (below the basement top) at all sites except U1350 (Fig. 6b). This relationship is consistent with vein formation

within an already cooled basement after cessation of hydrothermal activity and might reflect an increasing lithologic influence on fluid composition with increasing distance that the seawater had to travel through the basaltic host rock (increasing "leaching" time). It seems that the igneous rocks between ~40 and 140 m below basement top had slightly colder temperatures than the overlying tropical ocean water. This could be explained by basement cooling from the deeper parts of the respective (cone-shaped) edifices, extending into much greater (colder) water depth. A similar temperature decrease with depth was also observed in Hole 735B at Atlantis Bank, a gabbroic ridge bordering the eastern flank of the Atlantis-II Fracture Zone in the Indian Ocean, with slopes reaching down to deeper water depths (Von Herzen and Scott, 1991). Although the oxygen isotopic composition for Early Cretaceous deep water is not known, various proxy records indicate that the Earth experienced a cooling phase during the Late Jurassic/Early Cretaceous transition with evidence for subfreezing temperatures in the pole regions (Price, 1999) and proposed formation of cold deep water at higher latitudes that migrated to lower latitudes at the bottom of the ocean similar as it happens today (e.g., Wagreich, 2009). The alternative possibility that these high $\delta^{18}O$ veins formed much later when the ocean has cooled in the Cenozoic seems unlikely since benthic $\delta^{18}O$ ratios ≥1 are not reached before ~35 Ma when the seawater $^{87}Sr/^{86}Sr$ composition has reached ~0.7078. The respective samples, however, show increasing $\delta^{18}O$ values (colder temperatures) with decreasing Sr isotope ratios.

The oxygen isotope composition of those veins from Shirshov Massif (U1346) that describe a trend towards lower $\delta^{18}O$ values but at constant $^{87}Sr/^{86}Sr$ ratios could theoretically be explained if this edifice was initially exposed above the sea level and has experienced subaerial tropical weathering (calcite formed from meteoric water at equatorial latitudes during the Cretaceous records $\delta^{18}O$ values of c. -5‰, Hays and Grossman, 1991). However, no evidence for oxidative subaerial weathering or emplacement above sea level is found in the rocks from U1346 (Sager et al., 2010). It is therefore more likely that these veins reflect the severe alteration of their basaltic host rocks at Shirshov (being most extensive of all Shatsky sites). Intruded seawater in poor communication with the open ocean (see Fig. 4c) can become isotopically depleted in ^{18}O (which fractionates into secondary minerals) resulting in low $\delta^{18}O$ values of the calcite that precipitates from them (Anderson and Lawrence, 1976).

Since the least basement-influenced veins (highest $^{87}Sr/^{86}Sr$ ratios) from the Tamu (U1347), Ori summit (U1349), and Shirshov (U1346) sites formed at upper ocean (but not necessary surface) seawater temperatures (belemnite oxygen isotope values around zero are supposed to indicate a neritic habitat, Grossman, 2012) and still approach the global Sr isotope seawater composition at the assumed ages of 143, 134 and 128 Ma (Fig. 6a), these veins cannot be formed much later than their enclosing igneous rocks (probably within a few million years, see Fig. 5). Further evidence comes from calcite oxygen isotope composition from veins formed at Ori flank Site U1350 showing clear indication for hydrothermal influence (strongly decreasing

$^{87}Sr/^{86}Sr$ ratios with increasing precipitation temperature peaking at 25-30°C as seen in Fig. 6 a). Since hydrothermal activity is inherently linked to magmatic heat sources, these U1350 vein carbonates testify for an early precipitation age shortly after basement formation when it was still relatively warm. Although similar high temperatures could be reached at later times by conductive reheating after the basement is sealed from circulating ocean water by insulating sediments, the narrow trend of the U1350 veins in Fig. 6a projecting back to Early Cretaceous (~130-135 Ma) seawater Sr isotope composition (and also early Cretaceous seawater O isotope ratios), strongly supports an Early Cretaceous age.

5.4 Carbon isotope composition: does the vein composition record the first Oceanic Anoxic Event?

Although the stratigraphic record of $^{13}C/^{12}C$ is influenced by a number of factors linked directly to biological processes and the global carbon cycle (see Saltzman and Thomas, 2012 for overview), the $\delta^{13}C$ values of marine carbonates remained relatively constant over the Phanerozoic with values close to zero (relative to PDB). Occasionally occurring excursions of the marine $\delta^{13}C$ values to higher or lower levels are therefore of great palaeoceanographic interest and can be also used for stratigraphic correlation. A positive excursion of $\delta^{13}C$ in marine calcite through the upper Valanginian in the Early Cretaceous has been recognized at several sites worldwide including the central Pacific Ocean (e.g., Line et al., 1992). A period of relatively constant $\delta^{13}C$ values in the Berriasian and Lower Valanginian (expressed as

negative $\delta^{13}C$ in belemnite calcite) is followed by a rapid excursion to positive values in the Upper Valanginian, which is then followed by a gradual decline to values around zero in the Hauterivian and Barremian. Except for the hydrothermally influenced Site U1350 samples (see above), Shatsky's vein calcite $\delta^{13}C$ values reflect a similar pattern if plotted according to the proposed age relationship of their host lavas (Fig. 7). Whereas all Tamu U1347 vein samples have consistently negative $\delta^{13}C$ values, veins from Ori summit reach the most positive $\delta^{13}C$ values (with one exception), and Shirshov vein calcite shows intermediate values close to zero. The three U1349 vein samples from Ori summit with markedly positive $\delta^{13}C$ ranging from 0.9 to 1.9 could therefore record the Upper Valanginian excursion, also known as Weissert Event, which is linked to the first global Oceanic Anoxic Event (e.g., Weissert et al., 1998; Weissert and Erba, 2004). Taken together, the C isotope values of the Shatsky vein calcite cannot unambiguously constrain the age of calcite precipitation but are consistent with an Early Cretaceous formation and with the proposed age relationship of the drill sites.

6. Conclusions

Based on their elemental and isotopic composition, a dominant control of seawater chemistry on calcite composition is evident for the Shatsky Rise vein samples. Assuming that the highest (seawater-like) $^{87}Sr/^{86}Sr$ ratios at each drill site reflect contemporaneous seawater composition, vein precipitation between ~80 and 140 Ma is possible according to the Sr isotope seawater evolution curve (Fig. 5). This would

indicate a total crack-sealing duration over more than 60 myr. Even precipitation at much younger times (younger than ~70 Ma), when seawater $^{87}Sr/^{86}Sr$ was considerably higher, is theoretically possible but would require unrealistically strong bulk contributions (>3 to 10%) from basaltic, low Sr isotopic sources to keep the vein $^{87}Sr/^{86}Sr$ values in the observed range. The following lines of evidence, however, point to rather early carbonate precipitation for the majority of the investigated veins, shortly after basement formation:

1) The apparent increase of the highest $^{87}Sr/^{86}Sr$ ratios in vein calcite from each drill site mimics the increase of the global seawater $^{87}Sr/^{86}Sr$ signature in the early Cretaceous (Fig. 5) and is consistent with the proposed formation age relationship of the respective Shatsky Rise edifices.

2) The trends of increasing $^{87}Sr/^{86}Sr$ ratios with decreasing precipitation depth within basement observed in veins from all sites except U1350 (Fig. 4a) and with decreasing precipitation temperatures (Fig. 6a) extrapolate back to Early Cretaceous seawater $^{87}Sr/^{86}Sr$ and $\delta^{18}O$ ratios at the top of the basement.

3) The trend of decreasing $^{87}Sr/^{86}Sr$ ratios with increasing precipitation temperatures for Site U1350 veins (Fig. 6a) clearly indicates a hydrothermal contribution to vein precipitation within a still warm basement. For comparison: cooling models for normal oceanic crust predict a duration of ≤10 myr for the main phase of cooling (Wei and Sandwell, 2006).

4) Variation in C isotope composition of vein calcite between the three edifices is

consistent with vein formation during the Early Cretaceous by reflecting the prominent shift from negative to positive $\delta^{13}C$ values in the Valanginian epoch and subsequent return to pre-excursion values ("Weissert Oceanic Anoxic Event") (Fig. 7).

Taken together, we conclude that the investigated calcite veins most likely precipitated shortly or within a few millions years after the formation of the Shatsky Rise volcanic edifices. Such interpretation is consistent with previous suggestions that secondary carbonate formation largely occurs within ≤10 Myr (Staudigel et al., 1981; Coggon and Teagle, 2011) or <20 Myr (Gillis and Coogan, 2011) after oceanic crust formation.

As shown in several recent studies (Coggon et al., 2010; Rausch et al., 2013; Rausch et al., in prep.), the elemental and isotopic composition of calcite veins can be used to reconstruct past seawater compositions, providing that the veins have formed at ambient seawater temperatures or if the geochemical evolution of the fluid can be reconstructed (Coggon et al., 2010; Coggon and Teagle, 2011). For Shatsky, these conditions are best achieved at the Ori edifice summit (all veins from Site U1349) and, with some limitations, for Shirshow (some veins from Site U1346) and for at least one vein sample from Tamu (U1347A, 16R-5, 119-123 cm). The comprehensive Mg/Ca, Sr/Ca, trace element and isotopic composition reported for these samples can therefore be used for further palaeoceanographic studies at times shortly before,

during and after the first global oceanic anoxic event in the upper Valanginian (Weissert et al., 1998). On the other hand, the data also illustrate a complex formation history for carbonate veins in oceanic plateau basement with hydrothermal fluid circulation at one site (Ori flank) and possible evidence for exchange with colder (deeper?) water at other sites.

Acknowledgements

S.L. and J.G. equally contributed to the contents, ideas and interpretations of this study. We are grateful to D. Nürnberg for enabling oxygen and carbon isotope determinations and to Kirsten Werner and Lulzim Haxhiaj (all GEOMAR) for conducting the measurements. Ulrike Westernströer, Karen Bremer (University Kiel), Silke Hauff (GEOMAR), Jinhui Guo, Chaofeng Li (both IGGCAS), and Huiyan Suo and Jiehong Pang (both OUC) are greatly acknowledged for their assistance with trace element and isotopic measurements. John M. McArthur is thanked for providing his original LOWESS Sr seawater evolution data files. This work benefitted from discussions and advice from F. Böhm (GEOMAR) and from constructive and detailed reviews from two anonymous reviewers that have significantly improved this manuscript. This research used samples and data provided by the Integrated Ocean Drilling Program (IODP). Funding for this research was provided by the NSFC project (Grants 41325009 and 41190072), and the S863 key program (2009AA093401).

References

Alt, J.C., Teagle, D.A.H., 1999. The uptake of carbon during alteration of the oceanic crust. Geochimica et Cosmochimica Acta 63, 1527-1535.

Anderson, T.F., Lawrence, J.R. (1967). Satble isotope investigations of sediments, basalts, and authigenic phases from Leg 35 cores. Initial Reports of the Deep Sea Drilling Project 35, Wahington (.S. Government Printing Office), 497-505

Bach, W., Peucker-Ehrenbrink, B., Hart, S.R., Blusztajn, J.S., 2003. Geochemistry of hydrothermally altered oceanic crust: DSDP/ODP Hole 504B-Implications for seawater-crust exchange budgets and Sr- and Pb-isotopic evolution of the mantle. Geochemistry Geocphysics Geosystems 4, 8904. doi:10.1029/200GC000419.

Baertschi, P., 1967. Absolute ^{18}O content of standard mean ocean water. earth and Planetary Science Letters 31, 341-344.

Banerjee N.R., Honnorez J., 2004. Data report: low-temperature alteration of uper oceanic crust from the Ontong Java Plateau, Leg 192: Alteration and vein logs. In: Fitton, J.G., Mahoney, J.J., Wallace, P.J., and Saunders, A.D. (Eds.), Proceedings ODP, Scientific Results, 192: College Station, TX (Ocean Drilling Program), 1–8.

Bao, S.-X., Zhou, H.-Y., Peng, X-T., Ji, F.-W., Yoa, H.-Q., 2008. Geochemistry of REE and yttrium in hydrothermal fluids from the Endeavour segment, Juan de Fuca Ridge. Geochemical Journal 42, 359-370.

Brady, P.V., Gislason, S.R., 1997. Seafloor weathering controls on atmospheric CO_2 and global climate. Geochimica et Cosmochimica Acta 61, 965-997.

Burke, W.H., Denison, R.E., Hetherington, E.A., Koepnick, R.B., Nelson, N.F., Otto, J.B., 1982. Variation of seawater $^{87}Sr/^{86}Sr$ throughout Phanerozoic time. Geology 10, 516-519.

Coogan, L.A., 2009. Alterad oceanic crust as an inorganic record of paleoseawater Sr concentration. Geochemistry, Geophysics, Geosystems 10. doi:10.1029/2008GC002341

Coggon, R.M., Teagle, D.A.H., Cooper, M.J., Vanko, D.A., 2004. Linking basement carbonate vein compositions to porewater geochemistry across the eastern flank of the Juan de Fuca Ridge, ODP Leg 168. Earth and Planetary Science Letters 219, 111-128.

Coggon, R.M., Teagle, D.A.H., Smith-Duque, C.E., Alt, J.C., Cooper, M.J., 2010. Reconstructing past seawater Mg/Ca and Sr/Ca from mid-ocean ridge flank calcium carbonate veins. Science 327, 1114-1117.

Coggon, R.M. Teagle, D.A.H., 2011. Hydrothermal calcium-carbonate veins reveal past ocean chemistry. Trends in Analytical Chemistry 30(8), 1252-1268

Coplen, T.B., Kendall, C., Hopple, J., 1983. Comparison of stable isotope reference samples. Nature 197, 6779-6800.

de Villiers, S., Greaves, M., Elderfield, H., 2002. An intensity ratio calibration method for the accurate determination of Mg/Ca and Sr/Ca of marine carbonates by ICP-AES, Geochemistry, Geophysics, Geosystems *3(1)*, doi:10.1029/2001GC000169.

Frank, M., 2002. Radiogenic isotopes: Tracers of past ocean circulation and erosional input. Reviews of Geophysics 40, doi:10.1029/2000RG000094.

Geldmacher, J. van den Bogaard, P., Heydolph, K., Hoernle, K., The age of Earth's largest volcano: Tamu Massif on Shatsky Rise (northwest Pacific Ocean). International Journal of Earth Sciences (in press).

Gillis, K.M., Coogan, L.A., 2011. Secular variation in carbon uptake into the oceanic crust. Earth and Planetary Science Letters 302, 385-392.

Grossmann, E., 2012. Oxygen isotope stratigraphy, in: Gradstein, F.M., Ogg, J.G., Schmitz, M., Ogg, G. (Eds.), The Geological Time Scale. Elsevier, doi: 10.1016/B978-0-444-59425-9.00010-X.

Hathorne, E. C., Gagnon, A., Felis, T., Adkins, J., Asami, R., Boer, W., et al., 2013. Inter-laboratory study for coral Sr/Ca and other element/Ca ratio measurements. Geochemistry Geophysics Geosystems, doi:10.1002/ggge.20230

Hart, S.R., Staudigel, H., 1978, Oceanic crust: age of hydrothermal alteration. Geophysical Research Letters 5, 1009-1012.

Hays, P.D., Grossman, E.L., 1991. Oxygen isotopes in meteoric calcite cements as indicators of continental paleoclimate. Geology 19, 441-444.

Heaton, D.E., Koppers, A.A.P., 2014. Constraining the rapid construction of Tamu Massif at an ~145 Myr old triple junction, Shatsky Rise. Goldschmidt Conference, Sacramento, 2014, abstract 948

Heydolph, K., Murphy, D., Geldmacher, J., Romanova, I., Greene, A., Hoernle, K.,

Weis, D., Mahoney,J. 2014. Plume versus plate origin for the Shatsky Rise oceanic plateau (NW Pacific): Insights from Nd, Pb and Hf isotopes. Lithos 200-201, 49-63.

Hoernle, K., Tilton, G., 1991. Sr-Nd-Pb isotope data for Fuerteventura (Canary Islands) basal complex and subaerial volcanics: application to magma genesis and evolution, Schweizerische Mineralogische und Petrographische Mitteilungen 71, 5-21.

Jeandel, C., Delattre, H., Grenier, M., Pradoux, C., Lacan, F., 2013. Rare earth element concentrations and Nd isotopes in the Southwest Pacific Ocean. Geochemistry Geocphysics Geosystems14, doi:10.1029/GC004309.

Kim, S.-T., O'Neil, J.R., 1997. Equilibrium and nonequilibrium oxygen isotope effects in synthetic carbonates. Geochimica et Cosmochimica Acta61, 3461-3475.

Li, C.-F., Li, X.-H., Li, Q.-L., Guo, J.-H., Li, X.-H., Y, Y.-H., 2012. Rapid and precise determination of Sr and Nd isotopic ratios in geological samples from the same filament loading by thermal ionization mass spectrometry employing a single-step separation scheme. Analytica Chimica Acta, 727, 54-60.

Lini, A., Weissert, H., Erba, E., 1992. The Valanginian isotopic event: a first episode of greenhouse climate conditions during the Cretaceous. Terra Nova 4, 374-384.

Mahoney, J.J., Duncan, R.A., Tejada, M.L.G., Sager, W.W., Bralower, T.J., 2005. Jurassic–Cretaceous boundary age and mid-ocean-ridge–type mantle source for Shatsky Rise. Geology, 33(3), 185–188, doi:10.1130/G21378.1.

McArthur, J.M., Howarth, R.J., Bailey, T.R., 2001. Strontium isotope stratigraphy: LOWESS Version 3. Best-fit line to the marine Sr-isotope curve for 0 to 509 Ma and accompanying look-up table for deriving numerical age. Journal of Geology, 109, 155-169.

McArthur, J.M., Janssen M.M.M., Reboulet, S., Leng M.J., Thirlwall, M.F., van de Schootbrugge B., 2007. Palaeotemperatures, polar ice-volume, and isotope stratigraphy (Mg/Ca, $\delta^{18}O$, $\delta^{13}C$, 87Sr/86Sr): The Early Creatceous (Berriasian, Valanginian, Hauterivian). Palaeogeography, Palaeoclimatology, Palaeoecology 248, 391-430.

Mucci, A., Morse, J.W., 1983. The incorporation of Mg2+ and Sr2+ into calcite overgrowths: influences of growth rate and solution composition. Geochimica et Cosmochimica Acta 47, 217-233.

Nakanishi, M., Sager, W. W., Klaus, A., 1999. Magnetic lineations within Shatsky Rise, northwest Pacific Ocean: Implications for hot spot-triple junction interaction and oceanic plateau formation. Journal of Geophysical Research 104, 7539-7556.

Nozaki, Y., 2001. Rare Earth Elements and their Isotopes, in: Encyclopedia of Ocean Sciences, Thorpe, S.A., Turekian K.K. (Eds.). Elsevier Science Ltd, 2354-2366.

Okai, T., Suzuki, A., Kawahata, H., Terashima, S., Imai, N., 2002. Preparation of a new geological survey of Japan geochemical reference material: Coral JCp-1. Geostandards Newsletter: The Journal of Geostandards and Geoanalysis 26 (1), 95-99.

Peterman, Z.E., Hedge, C.E., Tourtelot, H.A., 1970. Isotopic composition of strontium in seawater throughout Phanerozoic time. Geochimica and Cosmochimica Acta 43, 105-120.

Price, G.D., 1999. The evidence and implications of polar ice during the Mesozoic. Earth Sciences Reviews 48, 183-210.

Price, G.D., Fözy, I., Janssen, N.M.M. Pálfy, J., 2011. Late Valanginian-Barremian (Early Cretaceous) paleotemperatures inferred from belemnite stable isotope and Mg/Ca ratios from Bersek Quarry (Gerecse Mountains, Transdanubian Range, Hungary). Palaeogeography, Palaeoclimatology, Palaeoecology 305, 1-9

Prokoph, A., Schileds, G.A., Veizer, J., 2008. Compilation and time-series analysis of a marine carbonate $\delta^{18}O$, $\delta^{13}C$, $^{87}Sr/^{86}Sr$ and $\delta^{34}S$ database through Earth history. Earth-Science Reviews 87, 113-133.

Rausch, S., Böhm, F., Bach, W., Klügel, A., Eisenhauer, A., 2013. Calcium carbonate veins in ocean crust record a threefold increase of seawater Mg/Ca in the past 30 million years. Earth and Planetary Science Letters 362, 215-224.

Rausch, S., Böhm, F., Bach, W., Klügel A., Eisenhauer, A., (in prep.) Trace elements in carbonate veins provide insights into seawater-ocean crust exchange.

Robinson, S.A., Vance D., 2009. The Nd-isotopic composition of late Cretaceous bathyal-abyssal seawater from fossil fish skeletal debris. Geophysical Research Abstracts 11, EGU General Assembly 2009

Sager, W.W., Kim, J., Klaus, A., Nakanishi, M., and Khankishieva, L.M.,1999. Bathymetry of Shatsky Rise, northwest Pacific Ocean: Implications for ocean plateau development at a triple junction. Journal of Geophysical Research 104, 7557-7576.

Sager, W.W., 2005. What built Shatsky Rise, a mantle plume or ridge processes?, in:

Foulger G.R., Natland, J.H., Presnall, D.C., Anderson, D.L. (Eds.), Plates, Plumes, and Paradigmas. Special Paer-Geological Society of America 388, 721-733.

Saltzman, M.R., Thomas, E., 2012. Carbon Isotope Stratigraphy. In: Gradstein, F.M., Ogg, J.G., Schmitz, M., Ogg, G. (Eds.), The Geological Time Scale. Elsevier, doi: 10.1016/B978-0-444-59425-9.00011-1.

Sager, W.W., Sano, T., Geldmacher, J., and the Expedition 324 Scientists, 2010. Proceedings IODP 324, Tokyo (Integrated Ocean Drilling Program Management International, INC.) doi:10.2204/iodp.proc.324.2010

Schrag, D. P., 1999. Rapid determination of high-precision Sr/Ca ratios in corals and other marine carbonates. Paleoceanography, 14, 97-102.

Staudigel, H., Hart, S.R., Richardson, S.H., 1981. Alteration of oceanic crust: processes and timing. Earth Planetary Science Letters 52, 311-327.

Taylor, S.R., McLennan, S.M., 1985. The continental crust: Its composition and evolution. Blackwell Scientific Publications, Oxford.

Terashima, S., Ando, A., Okai, T., Kanai, Y., Taniguchi, M., Takizawa, F., Itho, S., 1990. Elemental concentrations in nine new GSJ rock reference samples -sedimentary rock series-. Geostandards Newsletter 14, 1-5.

Tominaga, M., Evans, H.E., Iturrino, G., 2012. "Equator crossing" of Shatsky Rise?: New insights on Shatsky Rise tectonic motion from downhole magnetic architecture of the uppermost lava sequences at Tamu Massif. Geophysical Research Letters 39, L21301, doi:10.1029/2012GL052967.

Veizer, J., Al, D., Azmy, K., Bruckschen, P., Buhl, D., Bruhn, F., Carden, G.H.F., Diener, A., Ebneth, St., Godderis, Y., Jasper, t., Korte, C., Pawellek, F., Podlaha O.G., Strauss H., 1999. $^{87}Sr/^{86}Sr$, $\delta^{13}C$ and $\delta^{18}O$ evolution of Phanerozoic seawater. Chemical Geology 161 (1-3), 59-88.

Von Herzen, R.P., Scott, J.H., 1991. Thermal modeling for Hole 735B, in: Von Herzen, R.P., Robinson, P.T. et al. (Eds.), Proceedings of the Ocean Drilling Program, Scientific Results, Vol. 118, College Station, TX

Wagreich, M., 2009. Stratigraphic constraints for climate control of lower Cretaceous oceanic red beds in the Northern Calcareous Alps (Austria), in: Hu, X., Scott, R.W., Wagreich, M., Wang, C. (Eds.), Cretaceous Red Beds: stratigraphy, composition, origins, and Paleoceanographic and paleoclimatic significance. SEPM Special Publication 91, p.91-99.

Wei, M., Sandwell D., 2006. Estimates of heat flow from Cenozoic seafloor using global depth and age data. Tectonophysics 417, 325-335.

Weissert, H., Lini, A., Föllmi, K.B., Kuhn, O., 1998. Correlation of Early Cretaceous carbon isotope stratigraphy and platform drowning events: A possible link? Palaeogeography, Palaeoclimatology, Palaeoecology 137, 189-203.

Weissert, H., Erba E., 2004. Volcanism, CO_2 and palaeoclimate: A Late Jurassic-Early Cretaceous carbon and oxygen isotope record. Journal of the Geological Society 161, 695-702

Yang, Y.-H., Zhang, H.-F., Chu, Z.-Y., Xie, L.-W., Wu, F.-Y., 2010. Combined chemical separation of Lu, Hf, Rb, Sr, Sm and Nd from a single rock digest and precise and accurate isotope determinations of Lu–Hf, Rb–Sr and Sm–Nd isotope systems using Multi-Collector ICP-MS and TIMS. International Journal of Mass Spectrometry 290, 120-126.

Zhang, J., Nozaki, Y., 1996. Rare earth elements and yttrium in seawater: ICP-MS determinations in the East Caroline, Coral Sea, and South Fiji basins of the western South Pacific Ocean. Geochimica et Cosmochimica Acta 60, 4631-4644.

Figure captions:

Fig. 1: Location of IODP drill sites on Shatsky Rise from which veins were studied. Bathymetry after Sager et al. (2010) and magnetic anomalies after Nakanishi et al. (1999). Preliminary ages for Tamu and Ori Massifs from Geldmacher et al. (in press) and Heaton and Koppers (2014) respectively. Only contours above 5 km depth are shown for clarity (contour lines at 500 m intervals).

Fig. 2: Mg/Ca versus Sr/Ca for Shatsky calcite vein samples color-coded according to their oxygen isotope ratio (if available). Arrows indicating temperature dependence of concentration data are based on Coggon et al. (2004).

Fig.3: Rare Earth Elements and Y concentration of calcite veins from Shatsky Rise. Sample symbols are squares: Site U1347 (Tamu), circles: U1350 (Ori flank), diamonds: U1349 (Ori summit), triangles: U1346 (Shirshov). Seawater composition (x 1000 for better comparability) from Jeandel et al. (2013) (SE Pacific, Station GYR at 700 m depth) with Y value from Zhang and Nozaki (1996) (SE Pacific at 1000 m) and hydrothermal fluid (x 10) from Bao et al. (2008) (Juan de Fuca Ridge, Salut vent, endmember composition). All data normalized to Post-Archean Australien Shale (PAAS, Taylor and McLennan, 1985). Calcite sample U1349A 11R-5, which shows distinct negative Ce anomalie is indicated.

Fig. 4: $^{87}Sr/^{86}Sr$ ratios of calcite veins versus a) depths within igneous basement

(mbbc= meters below basement contact, calculated as distance to the top of igneous basement contact, i.e. the former volcano-seawater interface), b) Sr/Ca ratio, c) Ce/Ce* (=2xCe/(La+Pr) all normalized to PAAS), d) $^{143}Nd/^{144}Nd$. Binary mixing calculation (with tick marks indicating basement contribution in %) assuming igneous basement composition of $^{87}Sr/^{86}Sr$= 0.7030, $^{143}Nd/^{144}Nd$=0.5132, Nd= 10.54 ppm, Sr= 170 ppm (based on Heydolph et al.2014) and Cretaceous (~135 Ma) seawater composition of $^{87}Sr/^{86}Sr$= 0.7074 (McArthur et al, 2001), $^{143}Nd/^{144}Nd$=0.5124 (Robinson and Vance, 2009 for the Pacific basin), Nd= 0.0000028 ppm, Sr= 38 ppm (Coogan, 2009). The strongly rectangular shape of the mixing curve reflects the low concentrations of Nd in seawater, being several orders of magnitude less than Sr (Frank, 2002).

Fig. 5: Seawater Sr isotope evolution curve after McArthur et al. (2001) (LOWESS vers. 4:08/04). If the highest $^{87}Sr/^{86}Sr$ calcite ratios at each edifice reflect the purest seawater signal (and lower values at each respective site interaction with less radiogenic Sr from the volcanic basement), veins could have formed between ~80 and ~141 Ma (intersection of stippled lines with seawater Sr curve). If samples are arranged according to preliminary $^{40}Ar/^{39}Ar$ age determinations or assumed ages of host lavas (see text for details), the highest ratios at each site show a systematic increase with time that mimics the Sr isotopic increase of contemporaneous seawater between 143 and 128 Ma. $^{87}Sr/^{86}Sr_{in}$ of Shatsky lavas ≈ 0.7029, Heydolph et al. (2014). Analytical errors (2σ) are smaller than symbol size.

Fig. 6: Oxygen isotope composition of vein samples versus a) $^{87}Sr/^{86}Sr$ ratio and b) mbbc (meters below basement contact), defined as depth of individual carbonate vein sample within the formation measured in meter below basement top (basalt-ocean interface). Oxygen isotopic composition of Early Cretaceous (128, 134 and 143 Ma) low latitude seawater (surface to medium depth) from Grossman (2012) based on fossil belemnite data from Prokoph et al. (2008). Calcite precipitation temperatures are inferred based the equations of Kim and O'Neil (1997) for equilibrium precipitation (low concentration of Ca^{2+} and HCO^-_3) and nonequilibrium precipitation (high concentration of Ca^{2+} and HCO^-_3) using a $^{18}O/^{16}O$ ratio of V-SMOW (Vienna standard mean ocean water) of 2005.2 (Baertschi, 1976) and assuming a $\delta^{18}O$ value for Cretaceous seawater (in an non-glacial world) of -1‰ (e.g. Grossman, 2012). Applied conversion between V-PDB and V-SMOW according to Coplen et al. (1983). Since the precipitation rate of abiogenic carbonate is relatively low (Rausch et al., in prep.), it can be assumed that the pore fluids have approached isotopic equilibrium and therefore the slightly colder temperatures inferred from equilibrium precipitation appear more appropriate.

Fig. 7: $\delta^{13}C$ values of vein calcite versus stratigraphy based on MacArthur et al. (2007) using the same age relationship for the Shatsky drill sites as in Fig. 5. Grey field encircles belemnite calcite samples (grey dots) and 3-point mean average (black curve) from MacArthur et al. (2007) (for the Berriasian to Hauterivian) and belemnite

average from Price et al. (2011) (for the Barremian). Because of their neritic habitat, belemnite calcite is considered to best reflect average upper ocean (but not exclusively surface) water composition at approximately the same depth level as the young volcanic edifice tops (see text). WOAE= Weissert Oceanic Anoxic Event (e.g., Weissert and Erba, 2004).

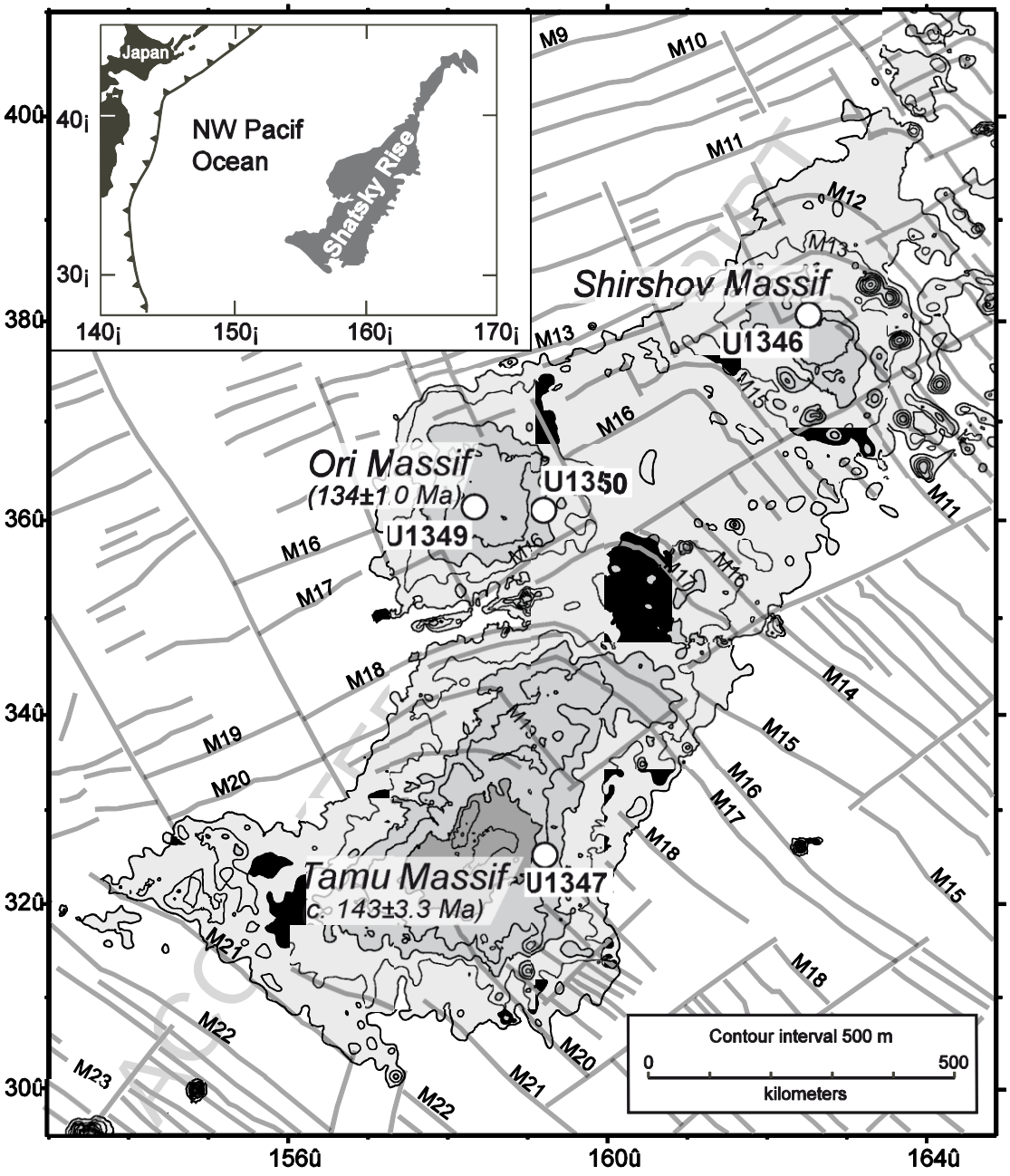

Fig. 1

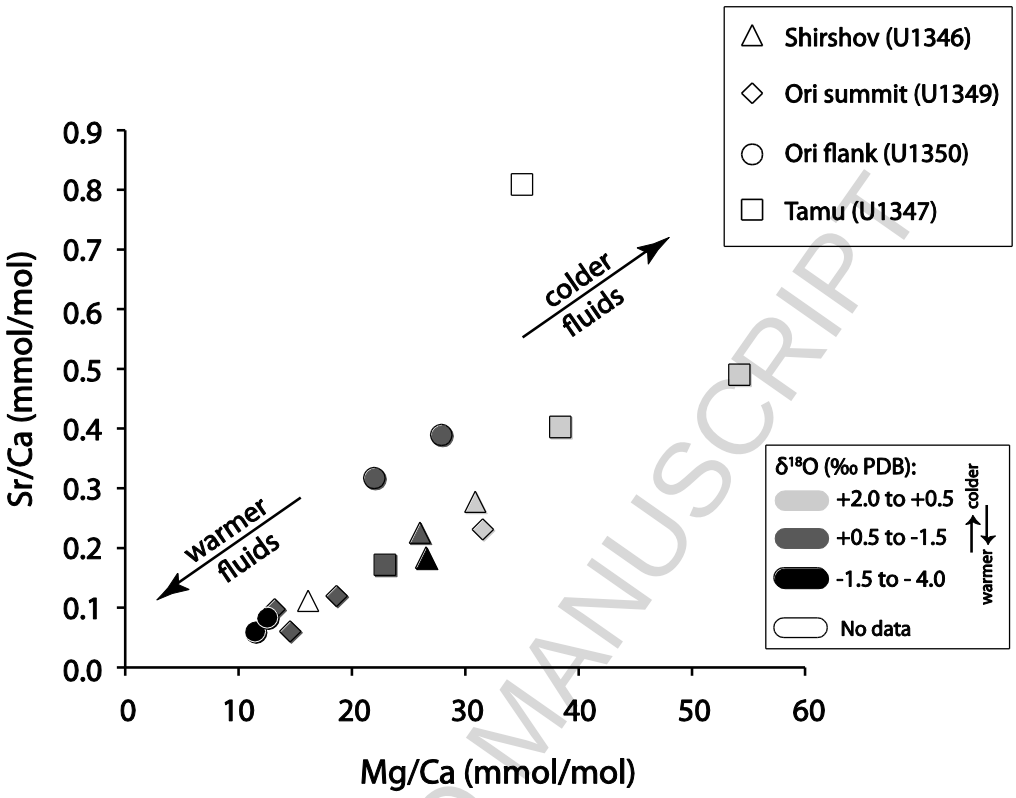

Fig. 2:

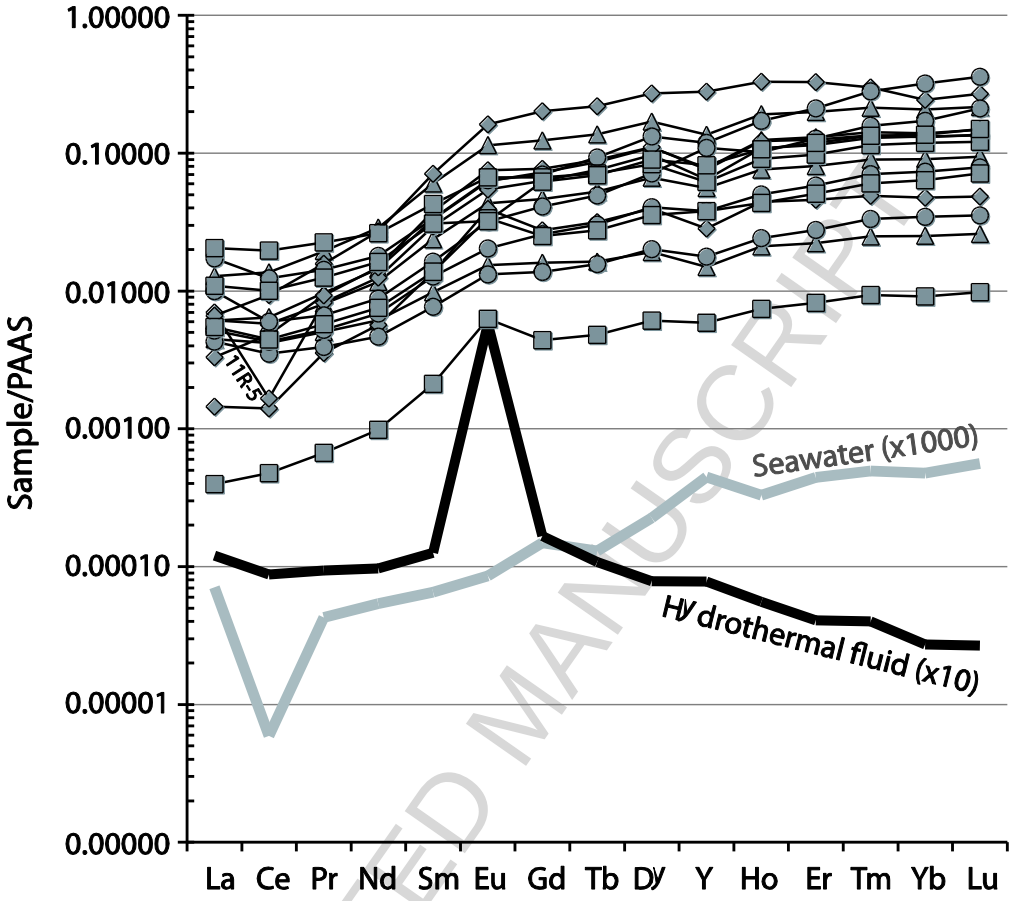

Fig.3

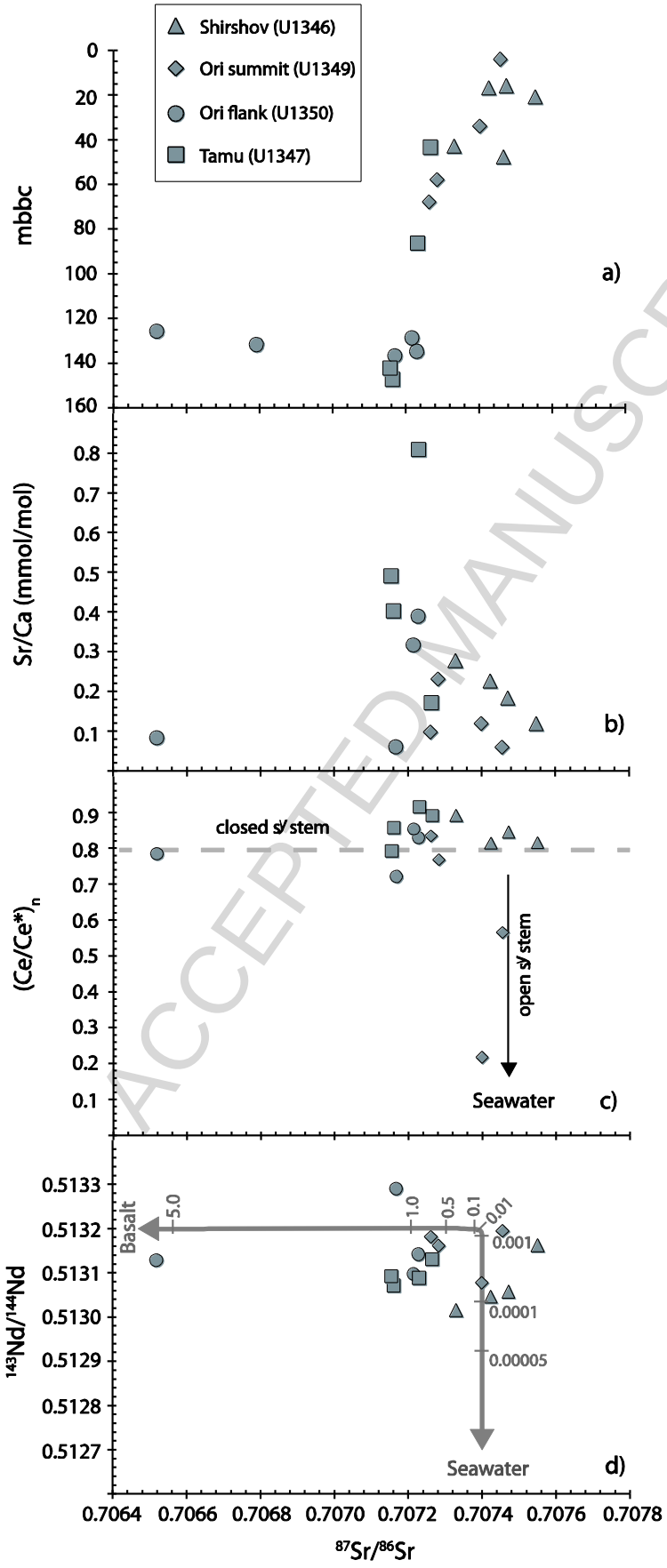

Fig. 4

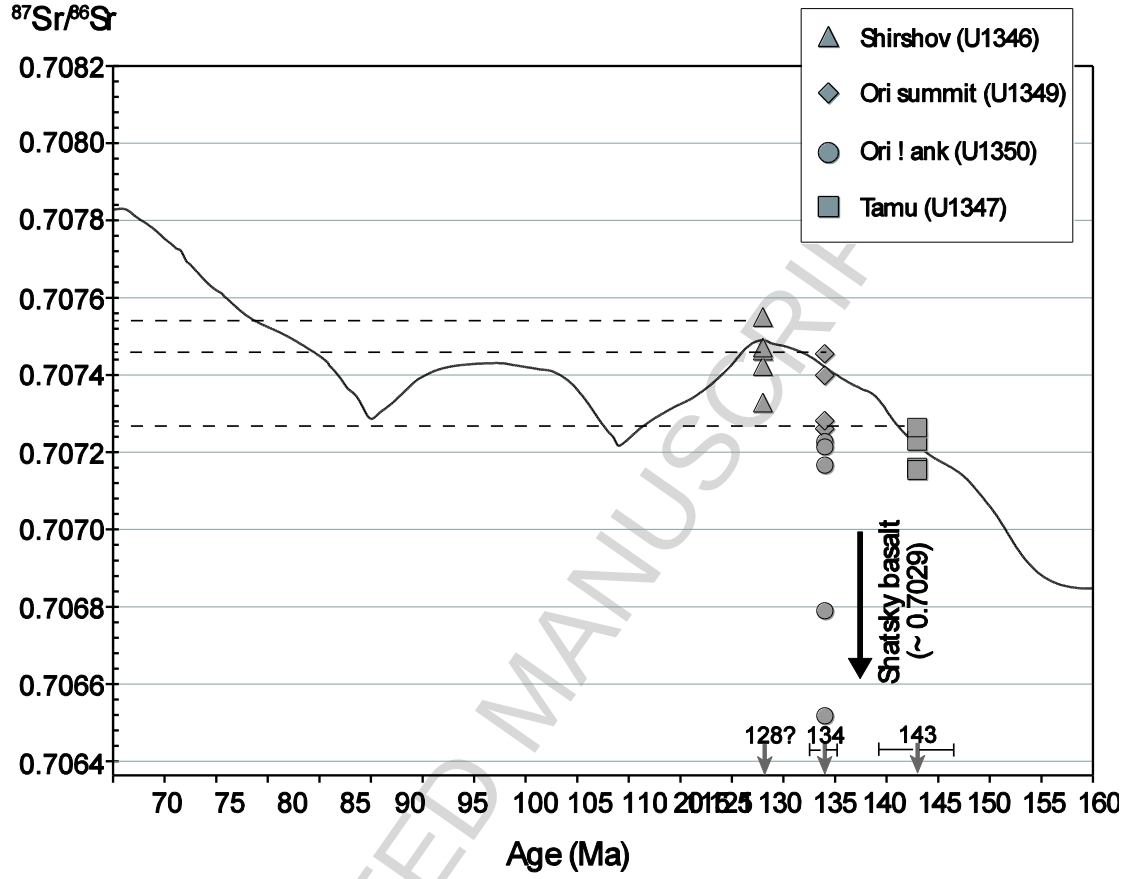

Fig. 5

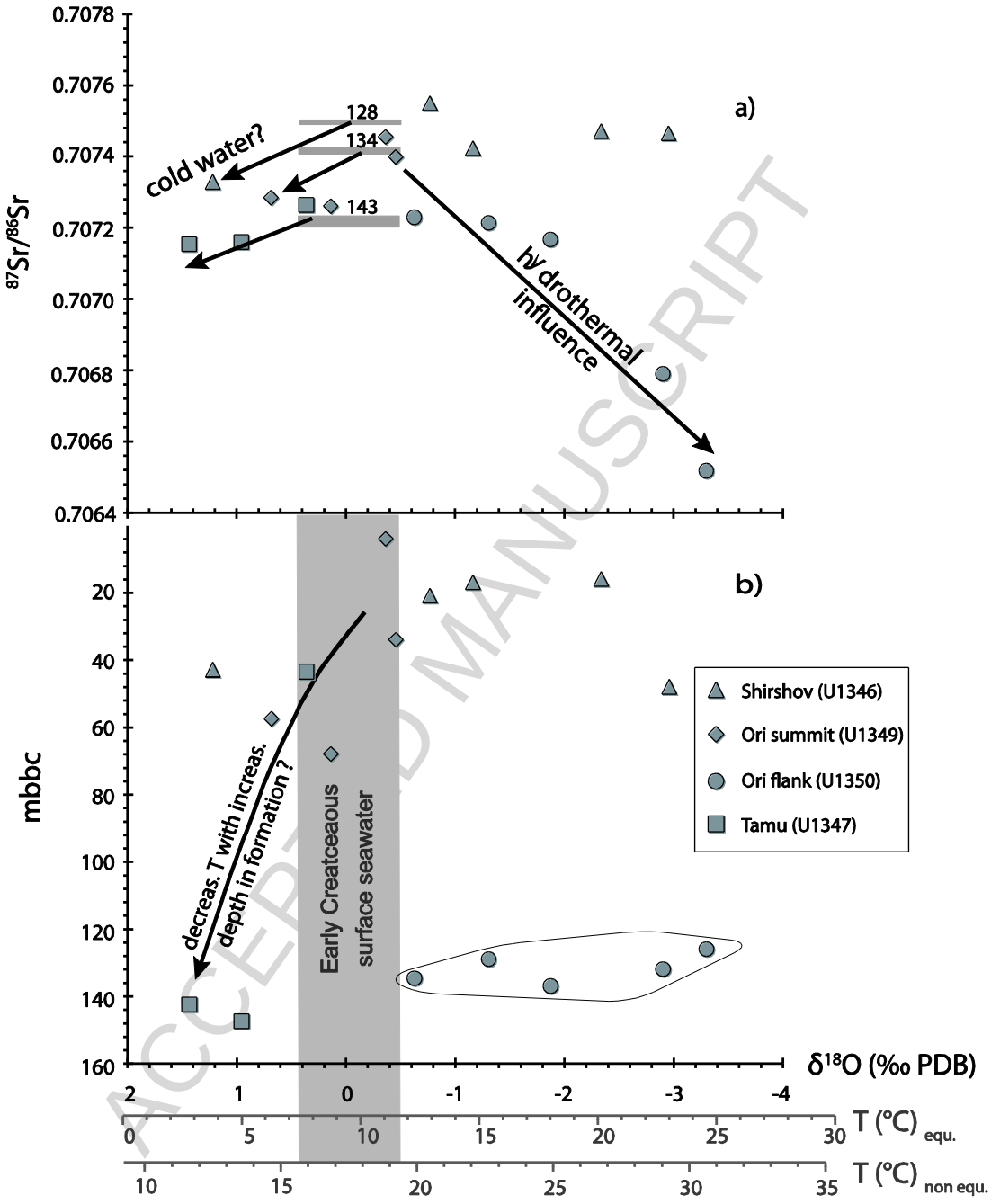

Fig. 6

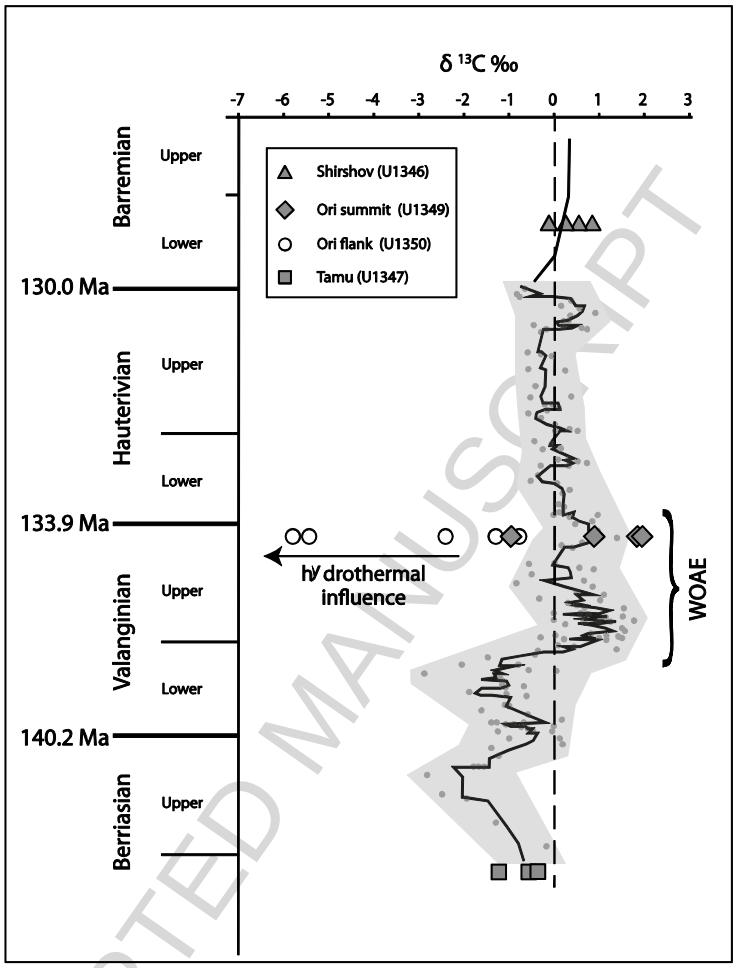

Fig. 7

Site,Hole	U1346A-	U1346A-	U1346A-	U1346A-	U1346A-	U1346A-	U1347A-	U1347A-	U1347A-	U1347A-
Core-Section	9R-2,	9R-2,	10R-2,	15R-1,	15R-1,	16R-1,	16R-5,	21R-2,	27R-6,	28R-4,
Interval (cm)	98-102 cm	136-144 cm	50-57 cm	10-16 cm	10-16cm Dupl	5.5-11 cm	119-123 cm	93-105 cm	82-89 cm	76-86 cm
mbbc	16	17	21	43	-	48	43	86	142	147
ICP-MS										
Li	0.39	0.98	0.73	2.15	2.44	n.d.	1.11	2.45	2.45	0.67
Sc	15.8	11.4	11.8	2.25	2.51	n.d.	0.42	0.82	1.03	0.60
Mn	7233	4757	1127	893	878	n.d.	5682	12272	7193	12155
Rb	0.82	1.13	0.16	0.60	0.70	n.d.	0.10	0.11	0.12	0.03
Sr	153	189	99.3	231	228	n.d.	143	620	358	304
Y	41.4	17.0	23.6	4.53	4.40	n.d.	1.79	18.7	11.6	24.8
Ba	0.60	1.07	0.87	3.01	3.46	n.d.	0.41	465	3.80	4.12
La	3.52	1.69	1.68	1.23	1.21	n.d.	0.11	5.62	1.51	2.99
Ce	7.74	3.29	3.66	2.38	2.38	n.d.	0.27	11.2	2.53	5.69
Pr	1.22	0.51	0.61	0.31	0.31	n.d.	0.04	1.41	0.36	0.78
Nd	6.76	2.73	3.40	1.44	1.44	n.d.	0.23	6.18	1.77	3.82
Sm	2.22	0.88	1.22	0.36	0.37	n.d.	0.08	1.58	0.51	1.14
Eu	0.81	0.31	0.44	0.11	0.11	n.d.	0.04	0.47	0.24	0.23
Gd	3.65	1.38	2.14	0.48	0.47	n.d.	0.13	1.98	0.74	1.84
Tb	0.67	0.26	0.42	0.08	0.08	n.d.	0.02	0.35	0.13	0.34
Dv	4.89	1.91	3.17	0.55	0.55	n.d.	0.18	2.40	1.03	2.59
Ho	1.15	0.46	0.75	0.13	0.12	n.d.	0.04	0.54	0.26	0.64
Er	3.38	1.37	2.21	0.38	0.37	n.d.	0.14	1.66	0.86	2.01
Tm	0.51	0.22	0.34	0.06	0.06	n.d.	0.02	0.27	0.14	0.32
Yb	3.38	1.48	2.26	0.41	0.40	n.d.	0.15	1.93	1.04	2.22
Lu	0.54	0.24	0.37	0.06	0.06	n.d.	0.02	0.30	0.18	0.37
Pb	0.99	0.57	2.20	0.23	0.32	n.d.	1.80	1.18	5.65	2.86
U	0.12	0.82	1.53	2.26	2.24	n.d.	0.04	0.00	2.14	0.22
Ce/Ce*	0.85	0.81	0.82	0.88	0.89	n.d.	0.89	0.91	0.79	0.86
ICP-OES										
Mg/Ca	26.5	26.0	16.1	30.5	30.9	n.d.	22.9	35.0	54.2	38.4
Sr/Ca	0.18	0.23	0.11	0.28	0.28	n.d.	0.17	0.81	0.49	0.40
$^{87}Sr/^{86}Sr$ (OU)			0.707540			0.707463(11	0.707264(13			0.707147(11
$^{87}Sr/^{86}Sr$ (G)	0.707471 (5)	0.707423 (6)	0.707560 (6)	0.707351 (8)	0.707329 (5)			0.707229 (6)	0.707154 (6)	0.707160 (5)

$^{143}Nd/^{144}Nd$	0.513057 (3)	0.513046 (4)	0.513162 (2)	0.513016 (5)	0.513016 (4)		0.513130 (6)	0.513088 (2)	0.513092 (2)	0.513071 (2)
δ 13C	0.24	0.81	0.81	0.55	-	-0.12	-0.42	n.d.	-0.57	-1.24
δ 18O	-2.34	-1.16	-0.77	1.22	-	-2.97	0.36	n.d.	1.44	0.96
T (°C) equ.	19.91	14.43	12.62	3.89	-	22.98	7.58	n.d.	2.97	5.01
T (°C) non equ.	26.70	21.89	20.29	12.56	-	29.38	15.84	n.d.	11.75	13.56

Site,Hole	U1349-	U1349-	U1349-	U1349-	U1349-	U1350A-	U1350A-	U1350A-	U1350A-	U1350A-
Core-Section	7R-4,	7R-4,	11R-5,	14R-1,	15R-2,	22R-2,	22R-4,	22R-6,	23R-1,	23R-3,
Interval (cm)	7.2-16 cm	7.2-16 cm Dupl.	72-75 cm	114-118 cm	87-91 cm	10-22 cm	106-110 cm	23-25 cm	80-86 cm	10-16 cm
mbbc	4	-	34	58	68	126	129	132	135	137
ICP-MS										
Li	0.42	0.25	1.65	2.96	0.22	0.26	0.30	n.d.	0.61	0.07
Sc	7.31	8.50	34.7	10.3	0.28	4.46	0.41	n.d.	0.63	1.65
Mn	78.5	76.2	211	990	5154	13298	7940	n.d.	9300	14623
Rb	0.12	0.13	2.14	1.29	0.03	0.05	0.02	n.d.	0.04	0.01
Sr	57.7	58.8	103	192	86.9	79.5	205	n.d.	306	57.0
Y	8.60	8.80	19.6	23.1	84.8	36.2	5.39	n.d.	11.5	33.2
Ba	0.17	0.21	6.78	0.57	0.07	0.31	1.25	n.d.	1.91	0.08
La	0.40	0.41	1.92	0.91	1.82	4.74	1.18	n.d.	1.42	2.74
Ce	0.80	0.83	0.94	2.75	5.29	7.01	1.99	n.d.	2.44	3.41
Pr	0.22	0.23	0.52	0.58	0.99	0.89	0.25	n.d.	0.33	0.42
Nd	1.33	1.37	2.93	3.49	6.35	4.22	1.09	n.d.	1.61	2.07
Sm	0.51	0.52	1.09	1.39	2.62	1.24	0.28	n.d.	0.47	0.60
Eu	0.28	0.28	0.39	0.53	1.15	0.45	0.09	n.d.	0.14	0.23
Gd	0.81	0.83	1.86	2.28	5.95	2.08	0.41	n.d.	0.76	1.21
Tb	0.15	0.16	0.37	0.44	1.07	0.45	0.08	n.d.	0.15	0.24
Dv	1.14	1.17	2.79	3.18	7.82	3.81	0.58	n.d.	1.17	2.05
Ho	0.27	0.27	0.65	0.73	1.98	1.03	0.14	n.d.	0.30	0.61
Er	0.78	0.80	1.95	2.13	5.56	3.60	0.47	n.d.	0.99	2.17
Tm	0.12	0.12	0.31	0.32	0.72	0.67	0.08	n.d.	0.17	0.38
Yb	0.77	0.80	2.15	2.12	3.97	5.21	0.56	n.d.	1.20	2.79
Lu	0.12	0.13	0.34	0.34	0.67	0.89	0.09	n.d.	0.20	0.53
Pb	0.16	0.18	0.24	0.53	0.29	1.39	0.41	n.d.	1.85	0.07
U	0.01	0.01	0.03	0.07	0.10	0.16	0.02	n.d.	0.02	0.01

Ce/Ce*	0.57	0.57	0.22	0.77	0.83	0.78	0.85	n.d.	0.83	0.72
ICP-OES										
Mg/Ca	14.4	14.6	18.6	31.6	13.2	12.5	22.0	n.d.	27.3	11.4
Sr/Ca	0.06	0.06	0.12	0.23	0.10	0.08	0.32	n.d.	0.39	0.06
$^{87}Sr/^{86}Sr$ (OU)							0.707214 (11)	0.706790 (11)		0.707167 (11)
$^{87}Sr/^{86}Sr$ (G)	0.707455 (7)		0.707399 (6)	0.707282 (6)	0.707261 (5)	0.706518 (7)			0.707227 (6)	
$^{143}Nd/^{144}Nd$	0.513195 (4)	0.513201 (4)	0.513078 (3)	0.513161 (5)	0.513181 (2)	0.513129 (2)	0.513097 (2)		0.513142 (6)	0.513290 (2)
δ 13C	1.91	-	1.84	0.87	-0.97	-0.78	-5.45	-1.30	-5.80	-2.41
δ 18O	-0.36	-	-0.46	0.68	0.14	-3.30	-1.31	-2.90	-0.63	-1.87
T (°C) equ.	10.79	-	11.21	6.22	8.57	24.59	15.09	22.64	12.01	17.74
T (°C) non equ.	18.68	-	19.05	14.63	16.71	30.79	22.47	29.08	19.75	24.80

Table 1 (continued)

Standard	ILS-1 (n=2)	ICP-1 (n=2)
ICP-MS		
Li	0.049	0.484
Sc	0.130	0.081
Mn	20.09	0.778
Rb	0.091	0.203
Sr	283.1	6563
Y	0.221	0.294
Ba	421.0	9.092
La	0.082	0.043
Ce	0.146	0.044
Pr	0.020	0.009
Nd	0.084	0.037
Sm	0.022	0.010
Eu	0.003	0.002
Gd	0.023	0.011
Tb	0.003	0.002
Dv	0.019	0.010
Ho	0.004	0.002
Er	0.013	0.007
Tm	0.002	0.001
Yb	0.013	0.009
Lu	0.002	0.002
Pb	0.149	0.180
U	1.539	2.384
ICP-OES		
Mg/Ca	15.5	4.1
Sr/Ca	0.34	8.68

Table 1: Values determined by ICP-MS are given in ppm. ICP-OES ratios are mmol/mol. OU= Ocean University, G= GEOMAR.

Highlights

- Chemical and isotopic composition of calcium carbonate veins in Early Cretaceous igneous basement at Shatsky Rise are used to constrain precipitation age.
- The Sr/Ca ratio of the vein calcite is positively correlated with Mg/Ca and both ratios generally decrease with increasing precipitation temperature.
- The correlation of decreasing Sr isotope ratios with increasing precipitation temperatures for some veins clearly indicates a hydrothermal origin.
- The combined trace element and isotopic data suggest a rather early carbonate precipitation for the majority of the veins, shortly after basement formation.